Amsterdam '14

We E106 15

Combining Diving and Reflected Waves for Velocity Model Building by Waveform Inversion

W. Zhou* (ISTerre, Université Grenoble Alpes), R. Brossier (ISTerre, Université Grenoble Alpes), S. Operto (Géoazur, CNRS, Université Nice Sophia-Antipolis) & J. Virieux (ISTerre, Université Grenoble Alpes)

SUMMARY

Full Waveform Inversion (FWI) aims to reconstruct high-resolution subsurface models from the full wavefield, which includes diving waves, subcritical reflections and short-spread reflections. Most of the successful applications of FWI have been driven by the information carried out by diving waves and subcritical reflections to build the long-to-intermediate wavelengths of the velocity structure. Alternative approaches have been recently revisited to retrieve this long-wavelength content from short-spread reflections only using some prior knowledge of the reflectivity. The present study presents a unified formalism, which aims to update the low wavenumbers of the velocity model by joint inversion of the diving waves and the full reflected wavefield. The method relies on an explicit scale separation between a smooth velocity macromodel and reflectivity, which is assumed to be known, and an explicit data separation between the short-spread reflections and the wide-angle arrivals (i.e., diving waves and subcritical reflections). Applications on simple layered models and a synthetic Valhall model show how the low-wavenumber content of the subsurface is emphasized at all depths by keeping only the transmission wavepaths generated by full wavefields in the gradient of FWI.

Introduction

Full Waveform Inversion (FWI) is an appealing method for quantitative high-resolution subsurface imaging (Virieux and Operto, 2009). FWI generally succeeds in recovering a broadband of wavenumbers in the shallow part of the targeted medium taking advantage of the broad scattering-angle provided by both reflected and diving waves. In contrast, deeper targets are often only illuminated by short-spread reflections, which favor the reconstruction of the short wavelengths at the expense of the longer ones, leading to a possible notch in the intermediate part of the wavenumber spectrum.

To update the velocity macromodel from reflection data, image-domain strategies (e.g., Symes and Carazzone, 1991) aim to maximize a semblance criterion in the migrated domain. Alternatively, recent data-domain strategies (e.g., Xu et al., 2012; Brossier et al., 2013; Ma and Hale, 2013), inspired by Chavent et al. (1994), rely on a scale separation between the velocity macromodel and prior knowledge of the reflectivity to emphasize the transmission regime in the sensitivity kernel of the inversion. However, all these strategies focus on reflected waves, discarding the low-wavenumber information carried out by diving waves.

With the current development of very long-offset and wide-azimuth acquisitions, a significant part of the recorded energy is provided by diving waves and subcritical reflections, and high-resolution tomographic methods should take advantage of all types of waves. We propose a unified formulation of FWI to update the low wavenumbers of the velocity model by the joint inversion of diving and reflected arrivals. We first explain the principles of our method and its efficient computer implementation. The method is formulated in the frequency domain for sake of compactness, although it is implemented in the time domain. Then, we analyse the contribution of each arrival in the data to the gradient of the modified FWI with two simple media, followed by considering the synthetic Valhall model.

Theory

Classical FWI considers the full data residual $\Delta d = d_{obs} - d$ in the misfit function, meaning

$$C_{classicalFWI} = 0.5\|\Delta d\|^2, \tag{1}$$

where observed and modeled data are denoted by d_{obs} and $d = Ru$, respectively (R samples the modeled wavefield u at receivers). Many strategies have been proposed to perform FWI of reflection data: they might differ in the misfit functions and/or in the domains in which the inversion is performed, but all rely on alternate update of reflectivity and velocity macromodel. Let's consider a simple one-reflector model with a single source-receiver couple and an initial model that generates residuals of the direct and reflected waves without cycle-skipping. The gradient of the classical FWI shows a wide first Fresnel zone, associated with the direct wave, and a secondary Fresnel zone, also known as migration isochrone, associated with the reflected wave (Fig. 1a). The high-wavenumber content of the migration isochrone prevents updating of long wavelengths in the deep part of the medium.

The decomposition of the subsurface model into a smooth background model m_0 and a high-wavenumber perturbation model δm leads to the wavefield decomposition into a background wavefield u_0 computed in m_0 and a wavefield perturbation δu scattered by δm, $u = u_0 + \delta u$. Assuming an initial guess of δm (through migration or impedance inversion for example), one can update m_0 by considering a misfit function focused on the reflected energy only (Xu et al., 2012; Brossier et al., 2013). For the one-reflector case, the corresponding gradient shows two low-wavenumber first Fresnel zones along the two-way reflected path, with a rabbit-ear shape (Fig. 1b).

One may include the direct/diving waves inside the norm definition of eq. (1), but this would inject the high-wavenumber isochrones into the FWI gradient through the correlation of u_0 with the backpropagated reflected field: this is not desirable for low-wavenumber imaging. This prompts us to explicitly separate the dataset associated with the direct/diving wave, $d_0 = Ru_0$, from the reflected dataset denoted by $\delta d = R\delta u$ in a new FWI misfit function

$$C_{newFWI} = 0.5\left(\|W_{d_0}\Delta d_0\|^2 + \|W_{\delta d}\Delta\delta d\|^2\right). \tag{2}$$

The benefit of C_{newFWI} is to filter out all the high-wavenumber isochrones generated by large-amplitude first-order scattered waves, while maintaining the contribution of both diving waves and short-spread reflected waves to update the long wavelengths. Weighting operators W_{d_0} and $W_{\delta d}$ allow us to balance the respective contribution of the diving waves and reflected waves. The gradient of (2) is derived with the Lagrangian formulation of the adjoint-state method:

$$\begin{aligned}\mathscr{L}(m_0,u_0,\delta u,d_0,\delta d,a_1,a_2,a_3,a_4) = C_{newFWI} + \langle a_1, B(m_0)u_0 - s\rangle \\ + \langle a_2, B(m_0+\delta m)\delta u - [B(m_0)-B(m_0+\delta m)]u_0\rangle + \langle a_3, Ru_0 - d_0\rangle + \langle a_4, R\delta u - \delta d\rangle \end{aligned} \quad (3)$$

where the forward-problem operator is denoted by B, the source term by s and the adjoint fields by a_i.

The adjoint wavefields are found by zeroing the partial derivatives of (3) with respect to the state variables u_0, δu, d_0 and δd. The field a_2, which satisfies $B(m_0+\delta m)^\dagger a_2 = -R^{\mathrm{T}} W_{\delta d}^{\mathrm{T}} W_{\delta d} \Delta\delta d^*$, can be decomposed into a background part λ_0^r computed in m_0 and a perturbation part $\delta\lambda^r$ scattered by δm. The field a_1, which satisfies $B(m_0)^\dagger a_1 = [B(m_0)-B(m_0+\delta m)]^\dagger a_2 - R^{\mathrm{T}}(W_{d_0}^{\mathrm{T}} W_{d_0}\Delta d_0^*)$, can be decomposed into a background part λ_0^d generated by the direct/diving-wave residuals Δd_0 and a scattered part $\delta\lambda^r$ associated with the back-propagation of the source term $[B(m_0)-B(m_0+\delta m)]a_2$ from reflectors. The superscript of fields λ denotes the type of adjoint source (direct/diving versus reflection residuals). The gradient of (2) is given by

$$\begin{aligned} G_{newFWI} &= \partial_{m_0}\mathscr{L} \approx a_1^\dagger\, \partial_{m_0} B\, u_0 + a_2^\dagger\, \partial_{m_0} B\, \delta u \\ &= \lambda_0^{d\dagger}\, \partial_{m_0} B\, u_0 + \delta\lambda^{r\dagger}\, \partial_{m_0} B\, u_0 + \lambda_0^{r\dagger}\, \partial_{m_0} B\, \delta u + \delta\lambda^{r\dagger}\, \partial_{m_0} B\, \delta u, \end{aligned} \quad (4)$$

where the adjoint operation is denoted by the symbol $\dagger$ and some terms appearing at $\delta m \neq 0$ positions have been neglected. The gradient of C_{newFWI} for the one-reflector case shows the superimposition of the first Fresnel zone associated with diving waves (first term in eq (4)), with the two first Fresnel zones along the two-way reflected path (second and third terms in eq. (4)). The fourth term in eq. (4) is associated to high-order scattering that should be non-zero but small-amplitude in practice.

A direct implementation of eq. (4) would require a scattered-field formulation of the forward problem, for which the source terms of the scattered fields δu and a_1 are expensive to compute in the time domain. To overcome this computational burden, we propose a cheaper implementation of G_{newFWI}.

$$G_{newFWI} = G_{classicalFWI \text{ in } m_0+\delta m} - \lambda_0^{r\dagger}\, \partial_{m_0} B\, u_0 = G_1 - G_2 \quad (5)$$

The workflow therefore includes three steps: [1] Compute the gradient G_1 of the classical misfit function $C_{classicalFWI}$ in the model $m_0+\delta m$ using weighted data residuals $W_{d_0}\Delta d_0 + W_{\delta d}\Delta\delta d$ instead of Δd in eq. (1). This term contains all the terms in eq. (4) plus high-wavenumber isochrones. [2] Compute the gradient G_2 of $C_{classicalFWI}$ in the model m_0 using only the weighted reflection residuals. This gives only high-wavenumber isochrones. [3] Subtract the two gradients. Note that step [1] and [2] can be performed in parallel.

High-order scattering effect and inversion parametrization

The proposed scheme is unable to suppress high-wavenumber isochrones generated by constructive correlation of multi-scattered wavefields. Fortunately, these isochrones have smaller amplitudes than those removed by our workflow ($\lambda_0^{r\dagger}\, \partial_{m_0} B\, u_0$ in eq. (5)). The gradient of the new misfit function, eq. (4), is shown in Fig. 1 for a two-reflector model. Each wavepath of this gradient represents the constructive interference between different wavefields, which undergo different orders of scattering during their propagation in $m_0+\delta m$ (Table 1). Most part of the high-order terms in the gradient will be cancelled out when multiple sources and receivers are considered, as they will not interefere constructively. Moreover, the footprint of these second-order high-wavenumber isochrones can be efficiently reduced by choosing a suitable subsurface parametrization for the gradient building. If the V_P gradient is built with the $V_P-\rho$ parameterization, a broadband of wavelengths are imaged according to the isotropic radiation pattern of V_P for this parameterization. In this case, the second-order high-wavenumber isochrones

cannot be filtered out (Fig. 1e). In contrast, if the $V_P - I_P$ parameterization is used, only the long-to-intermediate wavelengths of V_P are reconstructed from the wide scattering angles (Fig. 1f), while the short-to-intermediate wavelengths of the subsurface are mapped into the I_P model, according to the radiation pattern of these two parameter classes. The $V_P - I_P$ parameterization is therefore chosen in the following to reduce the imprint of the high-wavenumber isochrones in the V_P models.

Part	A	B	C	D	E	F
Interference (Scat. order)	$\lambda_0^d \star u_0$ (1)	$\delta\lambda_1^{r_1} \star u_0$ (2)	$\lambda_0^{r_1} \star \delta u_1$ (2)	$\delta\lambda_1^{r_1} \star \delta u_1$ (3)	$\delta\lambda_2^{r_2} \star u_0$ (2) $+\delta\lambda_{1,2}^{r_2} \star u_0$ (3)	$\lambda_0^{r_2} \star \delta u_2$ (2) $+\lambda_0^{r_2} \star \delta u_{1,2}$(3)

Part	G	H	I, J	K
Interference (Scat. order)	$\delta\lambda_1^{r_2} \star u_0$ (2)	$\lambda_0^{r_2} \star \delta u_1$ (2)	$\delta\lambda_1^{r_2} \star \delta u_1$ (3)	$\delta\lambda_2^{r_2} \star \delta u_2$ (3) + $\delta\lambda_2^{r_2} \star \delta u_{1,2}$ (4) + $\delta\lambda_{1,2}^{r_2} \star \delta u_2$ (4) + $\delta\lambda_{1,2}^{r_2} \star \delta u_{1,2}$ (5)

Table 1 *Wavepaths for the two-reflector case. Numbers in brackets indicate orders of missing scattering with respect to m_0. Superscript of λ denotes the type of residual in the adjoint source (diving wave (d), reflections from the first (r_1) or second (r_2) reflector). Subscript denotes the index of the reflector at which scattering occurs; 0: no scattering , 1 or 2: scattering at the first or second reflector, respectively, (1,2): successive scatterings at the first and second reflectors. Here, scattering includes both transmission and reflection at interfaces. † is ommited and $\star$ denotes the radiation pattern $\partial_{m_0} B$ for sake of compactness. See Fig. 1d for the graphical interpretation of these wavepaths.*

Numerical example in the synthetic Valhall model

We show FWI gradients that are computed in the synthetic 2D Valhall model (Fig. 2). Background velocity and impedance models are built by Gaussian smoothing and high-pass filtering of the true model, respectively. Sources and receivers are deployed on the surface and the offset range is limited within $\pm$2.19km. The new FWI gradient (Fig. 2g) is obtained by subtracting G_2 (Fig. 2f) from G_1 (Fig. 2e), eq. (5), using the weighted residuals in eq. (2). Comparison with the classical FWI gradient for V_P computed with the (V_P, ρ) parameterization and unweighted residuals (Fig. 2h) highlights how the low wavenumbers of the new gradient can be successfully updated in the deep part of the Valhall model, while maintaining the low-frequency contribution of the diving waves in the shallow part.

Conclusions and perspectives

We propose to build the velocity macromodel by FWI by joint inversion of diving waves and reflected waves. Our approach relies on the explicit decomposition of the subsurface model into a smooth background velocity model and reflectivity, and the dataset into diving waves and short-spread reflected waves. These decompositions make the velocity gradient to be dominated by surface-to-surface and reflector-to-surface first Fresnel zones. We propose a computationally efficient implementation of this approach by subtracting two gradients computed by classical FWI in two models, one with the prior reflectivity and one without. Although fictitious second-order isochrones cannot be explicitly suppressed, they are mostly removed by stacking over multiple sources and receivers. The role of the subsurface parameterization to drive the FWI toward the reconstruction of the long wavelengths is also highlighted.

Acknowledgments: This work is funded by the SEISCOPE consortium (*http://seiscope2.osug.fr*). This study is granted access to the HPC facilities of CIMENT (Université Joseph Fourier, Grenoble) and GENCI-CINES under grand 046091. Authors thank L. Métivier and Y. Li for fruitful discussions.

References

Brossier, R., Operto, S. and Virieux, J. [2013] Toward data-domain waveform inversion of reflected waves. *EAGE Technical Program Expanded Abstracts 2013*, Workshop F01.

Chavent, G., Clément, F. and Gòmez, S. [1994] Automatic determination of velocities via migration-based traveltime waveform inversion: A synthetic data example. *SEG Technical Program Expanded Abstracts 1994*, 1179–1182, doi: 10.1190/1.1822731.

Ma, Y. and Hale, D. [2013] Wave-equation reflection traveltime inversion with dynamic warping and full waveform inversion. *Geophysics*, **78**(6), R223–R233.

Symes, W.W. and Carazzone, J.J. [1991] Velocity inversion by differential semblance optimization. *Geophysics*, **56**, 654–663.

Virieux, J. and Operto, S. [2009] An overview of full waveform inversion in exploration geophysics. *Geophysics*, **74**(6), WCC1–WCC26.

Xu, S., Wang, D., Chen, F., Lambaré, G. and Zhang, Y. [2012] Inversion on reflected seismic wave. *SEG Technical Program Expanded Abstracts 2012*, 1–7, doi:10.1190/segam2012-1473.1.

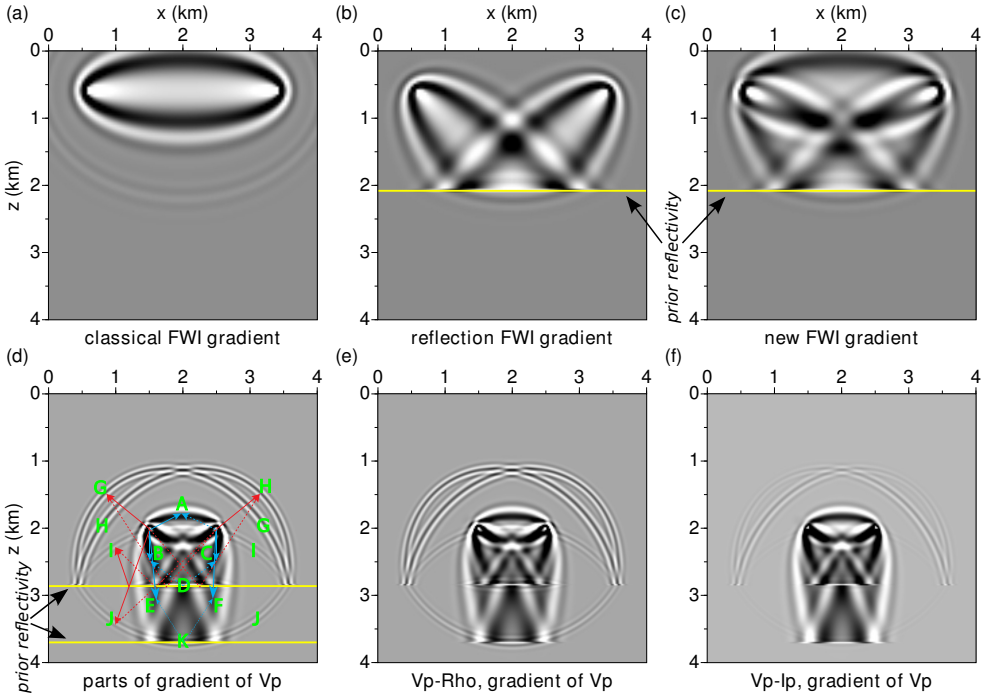

Figure 1 *(a-c) Gradients for one-reflector case. (a) Classical FWI, (b) Reflection FWI, (c) New FWI. (d-f) Gradients for two-reflector case. (d) Labeled wavepaths (Table 1). Solid and dash arrows denote the paths followed by the incident and adjoint wavefields, respectively. Blue paths are useful for long-wavelength updates unlike the red ones. New FWI gradient for (d) ($V_P - \rho$) parameterization and (f) ($V_P - I_P$) parameterization. Note how the unwanted high-order isochrones have been damped.*

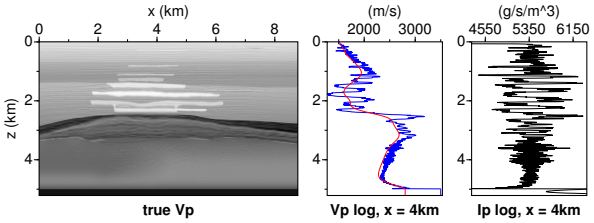

Figure 2 *(a) True Valhall model. (b-c) Log of the true and background V_P (b) and I_P (c).*

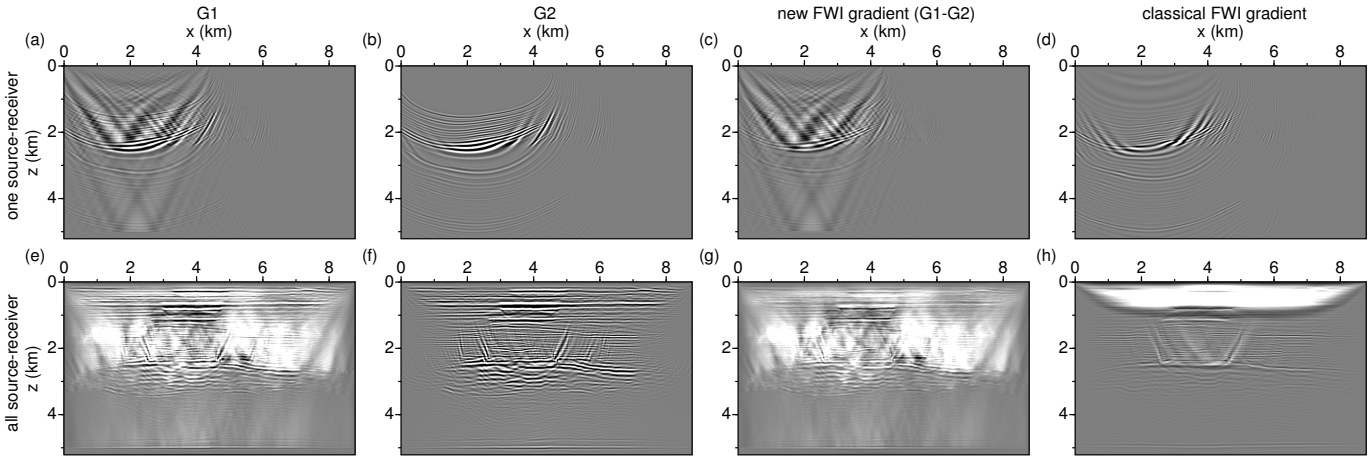

Figure 3 *Preconditioned gradients of V_P. (a-d) One source-receiver pair. (e-h) Full acquisition. (a,e) Classical FWI gradient computed with prior reflecitivity. (b,f) First-order isochrones computed without prior reflecitivity. (c,g) New FWI gradient. (d,h) Classical FWI gradient without residual weighting.*